Sigma-Delta Dynamic Receive Beamforming

D-L Donald Liu, Dan Brueske, Todd Willsie, Chris Daft
Siemens Medical Solutions USA, Inc., Ultrasound

Abstract An architecture is described for receive beamforming using sigma-delta conversion. The effects of signal stretching to achieve dynamic receive delays are analyzed and simulated. The presented architecture provides a simple and effective solution to the dynamic receive artifacts.

1. Background

Sigma-delta (abbreviated SD hereafter) conversion is an analog-to-digital conversion technology that utilizes oversampling and noise shaping. Oversampling refers to the fact that the sampling rate is much higher (e.g. 10 times or more) compared to the Nyquist sampling rate, while noise shaping refers to the use of few quantization bits (e.g. 1~4 bits) with the quantization noise energy being pushed away from the signal bandwidth in the spectral domain. For example, with a low-pass SD converter, the signal's spectral energy concentrates in the low frequency region while the spectral energy of quantization noise concentrates in the high frequency region. Subsequent digital filtering (e.g. low-pass filtering) is used to remove the quantization noise from the low-bitwidth data stream and reconstruct the signal with a higher bitwidth (see Figure 1).

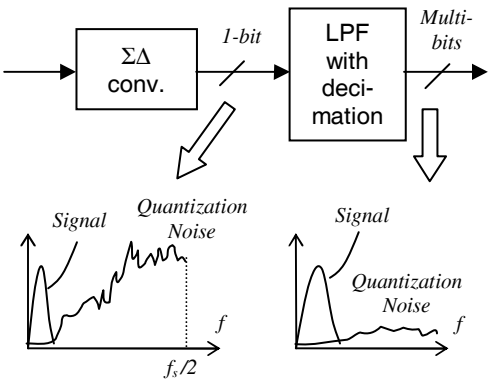

Figure 1. Sigma-delta (SD) conversion and digital low-pass filtering

SD conversion is an increasingly attractive technology for use with ultrasonic beamforming, due to the advancement of semiconductor manufacturing technology that leads to small line widths and high operating frequencies. The small time-delay quantization of SD conversion reduces and often eliminates the need for interpolation filters. In addition, SD conversion offers a trade-off between bandwidth and dynamic range that matches the needs of ultrasonic imaging in different modes.

However, dynamic receive beamforming commonly used in ultrasonic imaging disrupts the spectral shaping of quantization noise and causes a significant degradation in in-band signal-to-quantization-noise ratio (SQNR). This issue has been the subject of several papers and patents in recent years [1-3].

2. Methods

2.1 Architecture

A new signal processing architecture was developed to address this issue. After mixing to baseband and SD conversion, element signals are fed into a delay memory and dynamically decimated by LPF1 under the control of dynamic receive delays.

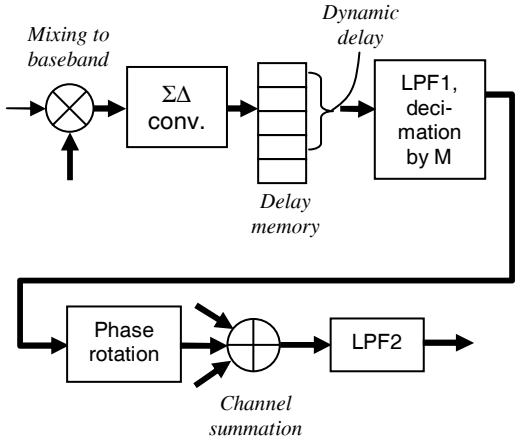

Figure 2. Baseband sigma-delta beamforming architecture

The conventional approach of direct sample repetition [1] can be viewed as the special case of LPF1=1 and decimation rate M=1, whereas the full sample reconstruction prior to channel summation [2] can be viewed as the special case of using LPF1 solely for reconstruction and LPF2=1. Since LPF1 is needed for every

channel, there's a strong motivation to make LPF1 as simple as possible, without severely degrading the in-band SQNR. One may speculate that the requirement on LPF1's performance is higher for more dynamic signal stretching and for higher requirements on SQNR.

2.2 Dynamic receive delay

The purpose of dynamic receive delay is to align waveforms generated at a focal point F as it moves outward. For simplicity, let's consider the 2-D geometry depicted in Figure 3 (the result is applicable to 3-D geometry). The 2-way propagation path length L is given by:

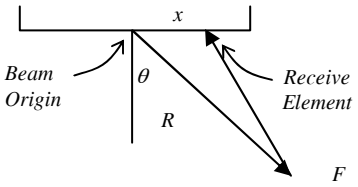

Figure 3. Geometry for computing dynamic delay

$$L = R + \sqrt{(R - x\sin\theta)^2 + x^2\cos^2\theta}$$
$$\approx 2R - x\sin\theta + \frac{x^2\cos^2\theta}{2R} \quad (1)$$
$$\frac{\partial L}{\partial(2R)} \approx 1 - \frac{x^2\cos^2\theta}{4R^2} \quad (2)$$

Eq. (2) shows that, as $2R$ increases uniformly with time, L increases at a slower rate (except for $x=0$, which corresponds to the element at the beam origin). Since channel signals are summed according to the value of L at each instant of time during dynamic receive focusing, a slower increase rate of L implies that signals are stretched by dynamic delay (a fact that can also be proven geometrically). The amount of stretching increases with element-beam origin distance x and decreases with range R and steering angle θ.

Let $R=ct/2$, $L=ct_1$, where t represents real time, and t_1 signifies the time instant at which a signal sample value is needed for computing beamsum, and let $R/(2x)$=Fnum, we get the following expression for stretching ratio:

$$\frac{\partial(t - t_1)}{\partial t} \approx \frac{\cos^2\theta}{16(\text{Fnum})^2} \quad (3)$$

For Fnum=1, the maximum stretching ratio is about 1/16th or 6.3%, while for Fnum=2, the maximum stretching ratio is 1/64th or 1.6%.

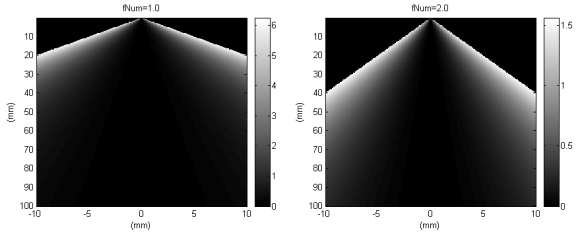

Figure 4. Plots of signal stretching ratio

Figure 4 shows example plots of signal stretching ratio, for Fnum=1 and 2, with an aperture size of 20 mm and an imaging range of 100 mm.

2.3 Analysis of dynamic decimation

With SD conversion, signals are typically sampled at a rate much higher compared to the Nyquist sampling rate. Normal (uniform) decimation by M applies a FIR filter (corresponding to the LPF1 filter in Figure 2) on the SD sequence with a step size of M, whereas dynamic decimation (which effectively stretches the signal, as discussed above) applies the filter with a step size less than or equal to M but treat the result as if the filter had been applied with a step size of M. For example, if the decimation filter is applied with a step size of M-1, then the signal would have been effectively stretched by a ratio of 1/M. Conceptually, one can achieve the same effect by applying the filter on the SD sequence sample by sample, then repeating every (M-1)th sample in the output (thereby growing the signal in length), and then uniformly decimating the result by M. By examining the spectra during the conceptual intermediate step where the samples have been repeated but before decimation, we can study the impact of sample repetition with filtering by LPF1.

2.4 Simulation Method

The following steps are followed:
Step 1. A Gaussian pulse with a specified center frequency f_0 and -6 dB bandwidth bw is computed at a sampling rate f_s (200 MHz). Two cases have been considered, with (f_0, bw)=(2.63, 1.56) MHz and (10, 6.25) MHz, respectively. These are representative of low and high operating frequencies of medical ultrasound. The corresponding oversampling ratios relative to signal bandwidths are 128 and 32, respectively.
Step 2. The pulse is convolved with a Gaussian random sequence, sampled at f_s and is about 200 cycles long at f_0. The result of convolution is normalized to have an rms amplitude of 0.15

to keep the signal amplitude within the range of about ±0.5, where ±1 corresponds to the full input range of the SD converter.

Step 3. Two small random noise sequences are added to the result of Step 2 to provide perturbation and simulate 2 different input signals. The amplitude of the random sequences is at least 10 dB below the quantization noise level.

Step 4. The signals are mixed to baseband using quadrature square-wave mixing.

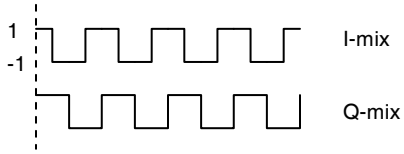

Figure 5. Quadrature square-wave mixing signals

Step 5. The complex signal after mixing is converted by a pair of 2nd-order low-pass sigma-delta converters, with H_∞ set at 1.5 [4].

Step 6. The result of Step 5 is passed through an LPF1, which is a 3rd-order comb filter with the following transfer function:

$$C(z) = \left(\frac{1}{M} \frac{1 - z^{-M}}{1 - z^{-1}} \right)^3$$
$$\left| C(e^{j\omega}) \right| = \left| \frac{\sin(M\omega/2)}{M \sin(\omega/2)} \right|^3 \qquad (4)$$

Two values of M have been considered: 8 or 16. The corresponding time-domain responses of the comb filter are 22 6-bit taps or 46 8-bit taps. For comparison, Step 6 is skipped to simulate the case of LPF1=1.

Step 7. The signals are stretched uniformly by repeating one sample for every 16 or 64 samples, which corresponds to the maximum stretching for realizing dynamic receive f-numbers of 1 or 2, as shown by Eq. (3). They are then decimated by 8, 16, or 1, depending on which filter was used as LPF1.

Step 8. The signal s and quantization noise n are estimated using the following:

$$\begin{cases} s = (s_1 + s_2)/2 \\ n = (s_1 - s_2)/\sqrt{2} \end{cases} \qquad (5)$$

where s_1 and s_2 are the results of Step 7.

Step 9. An LPF2 is applied separately to s and n. The spectral response of LPF2 is Gaussian centered at DC with a -6 dB bandwidth equal to the signals bandwidth bw used in Step 1.

Step 10. The SQNR is estimated as

$$20*\log_{10}[\ \mathrm{rms}(s) / \mathrm{rms}(n)\ ]$$

where s and n are after the filtering described in Step 9 and rms(·) stands for computing the root-mean-square amplitude of the sequence.

3. Results

Signal spectra under various processing conditions are shown below.

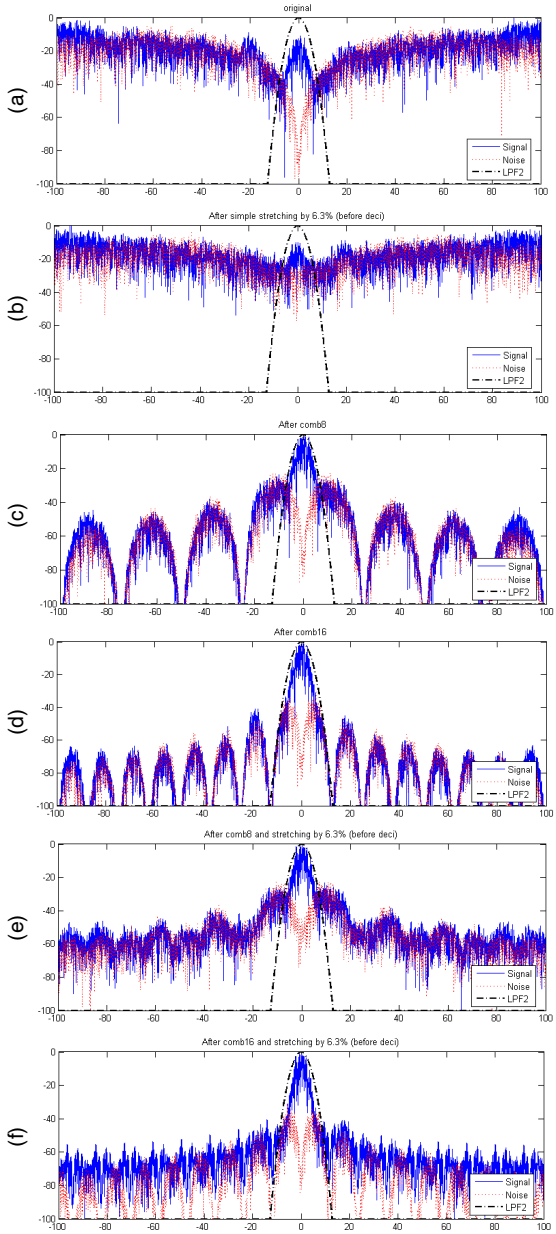

Figure 6. Representative spectra for the wide-band simulation with f_0=10 MHz and bw=6.25 MHz.

In Figure 6, (a) shows the spectra of baseband SD conversion and illustrates the effects of spectral shaping; (b) shows the effect of direct sample repetition (one repetition for every 16 samples was used here), where we see that spectral shaping is nearly wiped out; (c) and (d) show the effects of applying a comb filter with M=8 and 16, respectively, where we see that spectral valleys are created by the filtering; (e) and (f) show the effect of sample repetition after applying the M=8 and M=16 comb filters, respectively, where we see that the in-band noise shaping is preserved (more so in (f) than in (e)), and that the valleys are filled up. The spectral valleys are important because after decimation, these frequency components alias into the signal passband, which affects particularly the noise amplitude since it's much lower compared to the signal amplitude.

The same processing as described in Section 2.4 is repeated 100 times using different realizations of the random sequences. The average in-band SQNR are summarized in Table 1. The standard deviation of SQNR is around 0.4 dB.

Table 1. In-band SQNR under various conditions

Oversampling ratio (OSR)	32			128			
SQNR after SD conversion (original)	37.7			67.6			(dB)
Rx Fnum	1	2	∞	1	2	∞	
Maximum signal stretch rate	6.3%	1.6%	0	6.3%	1.6%	0	
Direct sample repetition	10.9	16.2	37.7	16.7	22.4	67.6	(dB)
Repetition after comb & deci by 8	35.4	37.5	38.6	45.7	52.1	67.7	(dB)
Repetition after comb & deci by 16	39.6	40.1	40.2	61.6	62.3	67.8	(dB)

4. Discussion

As shown in Figure 6 and Table 1, direct sample repetition causes a significant degradation of in-band SQNR. For example, with oversampling ratio being 32, the in-band SQNR is significantly reduced from the original of 37.7 dB to 10.9 and 16.2 dB, for rx f-number of 1 and 2, respectively.

With comb filtering, the SQNR degradation due to dynamic receive focusing is much reduced. For a higher oversampling ratio (OSR), a longer comb filter is required to maintain the SQNR. For example, with OSR being 32, a comb8 filter (M=8) causes an SQNR loss of 2.3 dB and 0.2 dB, for rx f-number of 1 and 2, respectively. However, when OSR is raised to 128, the comb8 filter still caused 21.9 and 15.5 dB of loss in SQNR, for rx f-number of 1 and 2, respectively, whereas with a comb16 filter, SQNR losses are correspondingly reduced to 6.0 and 5.3 dB.

It is noteworthy that the simulated cases assumed a constant stretching ratio over the entire signal record length. In actual dynamic receive focusing, however, as shown by Eq. (2) and Figure 4, the stretching ratio is range dependent and is inversely proportional to R^2. Therefore, for a fixed element location (with a fixed x value), the stretch ratio goes down from the value given by Eq. (3), so the SQNR values shown in Table 1 represent the worst cases.

It is of interest to note that in some cases the SQNR after comb filtering and sample repetition is higher than the original value. This happens when the comb filter's passband is comparable to signal's passband. For example, with f_s=200 MHz and M=16, the comb filter's -6 dB bandwidth is 9.17 (MHz) based on Eq. (4). This is comparable to the signal's bandwidth (6.25 MHz) with OSR=32. Therefore, the gain in SQNR is at the expense of some loss in signal bandwidth.

In summary, the presented architecture provides a simple and effective solution to the dynamic receive artifacts associated with sigma-delta conversion.

5. References

[1] S. R. Freeman, et al, IEEE UFFC vol. 46, no. 2, 1999.
[2] H.-S. Han, et al, Proc. IEEE US Symp., 2006, pp. 2140-2143.
[3] D.-L. Liu, et al, US Patent App., 2007
[4] R. Shreier and G. C. Temes, "Understanding sigma-delta converters", John Wiley & Sons, 2005.